

This is an Open Access document downloaded from ORCA, Cardiff University's institutional repository:<https://orca.cardiff.ac.uk/id/eprint/109104/>

This is the author's version of a work that was submitted to / accepted for publication.

Citation for final published version:

Cattaneo, Stefano, Freakley, Simon, Morgan, David , Meenakshisundaram, Sankar , Dimitratos, Nikolaos and Hutchings, Graham 2018. Cinnamaldehyde hydrogenation using Au-Pd catalysts prepared by sol immobilisation. *Catalysis Science and Technology* 8 , pp. 1677-1685. 10.1039/C7CY02556D

Publishers page: <http://dx.doi.org/10.1039/C7CY02556D>

Please note:

Changes made as a result of publishing processes such as copy-editing, formatting and page numbers may not be reflected in this version. For the definitive version of this publication, please refer to the published source. You are advised to consult the publisher's version if you wish to cite this paper.

This version is being made available in accordance with publisher policies. See <http://orca.cf.ac.uk/policies.html> for usage policies. Copyright and moral rights for publications made available in ORCA are retained by the copyright holders.



## Supporting Information

# Cinnamaldehyde hydrogenation using Au-Pd catalysts prepared by sol immobilisation

Stefano Cattaneo, Simon J. Freakley, David J. Morgan, Meenakshisundaram Sankar, Nikolaos Dimitratos, and Graham J. Hutchings\*

---

*Cardiff Catalysis Institute, School of Chemistry, Cardiff University, Cardiff, CF10 3AT, United Kingdom.*

\* Hutch@cardiff.ac.uk

**Table S1.** MP-AES and XPS quantification analysis of the  $\text{Au}_x\text{Pd}_y$  catalysts.

Catalyst	Metal loading (wt %)	Au/Pd ratio (mol/mol)			Binding energy (eV)	
		Theoretical	MP-AES	XPS	$\text{Au}4f_{7/2}$	$\text{Pd}3d_{5/2}$
$\text{Au}_{100}\text{Pd}_0/\text{TiO}_2$	0.94	100 : 0	100 : 0	100 : 0	83.5	-
$\text{Au}_{95}\text{Pd}_5/\text{TiO}_2$	1.00	95 : 5	96 : 4	92 : 8	83.7	335.0
$\text{Au}_{65}\text{Pd}_{35}/\text{TiO}_2$	0.92	65 : 35	68 : 32	64 : 36	83.4	334.9
$\text{Au}_{50}\text{Pd}_{50}/\text{TiO}_2$	1.00	50 : 50	47 : 53	54 : 46	83.4	335.0
$\text{Au}_{35}\text{Pd}_{65}/\text{TiO}_2$	0.96	35 : 65	39 : 61	36 : 64	83.2	335.0
$\text{Au}_0\text{Pd}_{100}/\text{TiO}_2$	0.98	0 : 100	0 : 100	0 : 100	-	335.0

**Figure S1.** Particle size distribution of (a) Au/TiO<sub>2</sub> (b) Au<sub>95</sub>Pd<sub>5</sub>/TiO<sub>2</sub> (c) Au<sub>65</sub>Pd<sub>35</sub>/TiO<sub>2</sub> (d) Au<sub>50</sub>Pd<sub>50</sub>/TiO<sub>2</sub> (e) Au<sub>35</sub>Pd<sub>65</sub>/TiO<sub>2</sub> (f) Pd/TiO<sub>2</sub>.

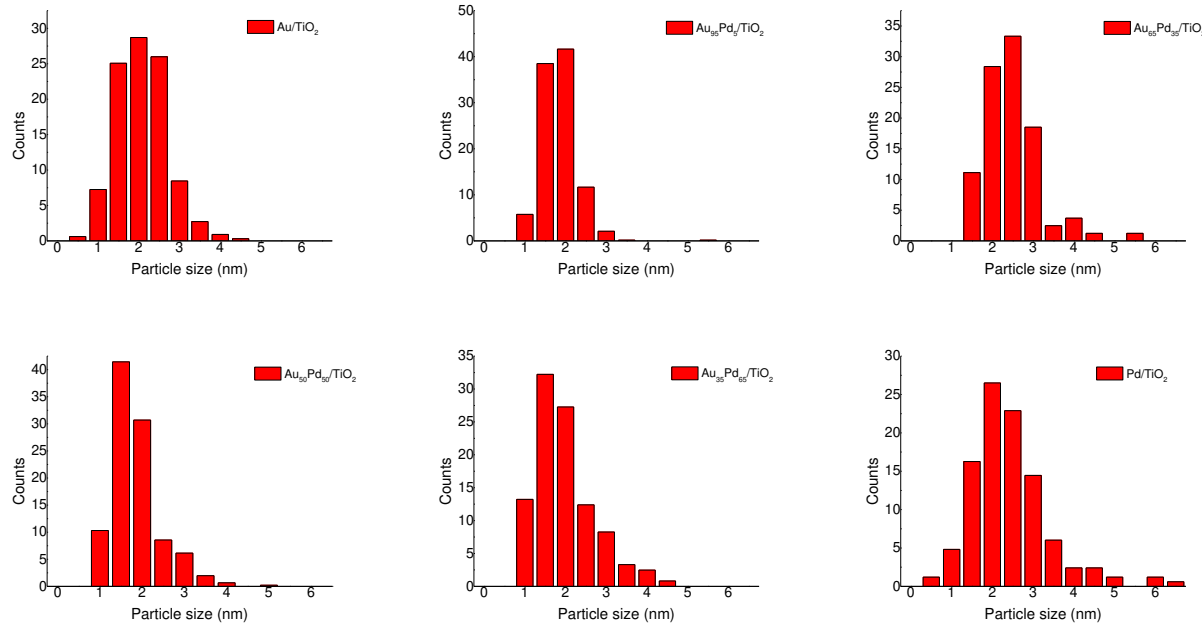


**Table S2.** Mean and median values (nm) obtained by TEM of the supported monometallic and bimetallic catalysts.

Au/TiO <sub>2</sub>		Au <sub>95</sub> Pd <sub>5</sub> /TiO <sub>2</sub>		Au <sub>65</sub> Pd <sub>35</sub> /TiO <sub>2</sub>		Au <sub>50</sub> Pd <sub>50</sub> /TiO <sub>2</sub>		Au <sub>35</sub> Pd <sub>65</sub> /TiO <sub>2</sub>		Pd/TiO <sub>2</sub>	
Mean	2.4	Mean	2.1	Mean	2.7	Mean	2.1	Mean	2.3	Mean	2.7
Std-dev	0.7	Std-dev	0.4	Std-dev	0.7	Std-dev	0.6	Std-dev	0.8	Std-dev	1.0
Median	2.3	Median	2.0	Median	2.6	Median	2.0	Median	2.1	Median	2.5

**Figure S2.** (i) Typical XRD pattern of a AuPd/TiO<sub>2</sub> catalyst in the 10-80 2 Theta (°) range, and (ii) of (a) Au<sub>100</sub>Pd<sub>0</sub>/TiO<sub>2</sub> (b) Au<sub>95</sub>Pd<sub>5</sub>/TiO<sub>2</sub> (c) Au<sub>65</sub>Pd<sub>35</sub>/TiO<sub>2</sub> (d) Au<sub>50</sub>Pd<sub>50</sub>/TiO<sub>2</sub> (e) Au<sub>35</sub>Pd<sub>65</sub>/TiO<sub>2</sub> (f) Au<sub>0</sub>Pd<sub>100</sub>/TiO<sub>2</sub> in the 40-48 2 (°) Theta range. It is possible to notice a single peak typical of alloy formation that shifts in the range 44-45 2-Theta (°) with variation of the Au/Pd molar ratio.

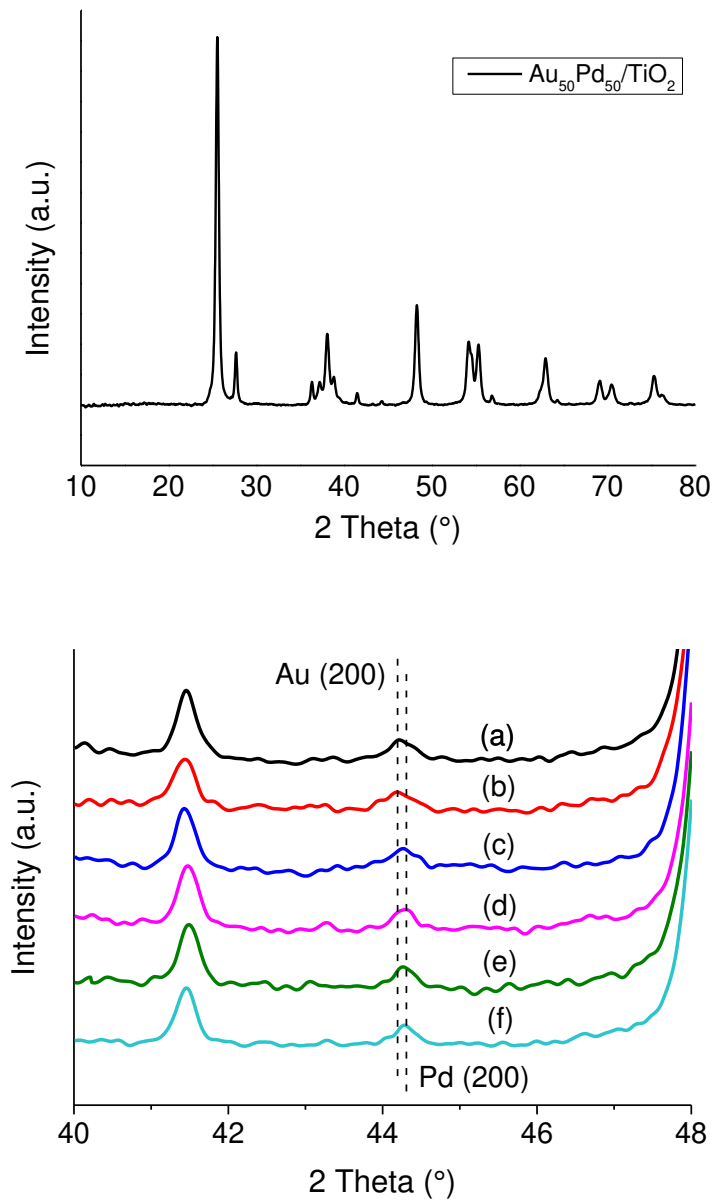


**Table S3.** Surface area and pore volume for the bare support ( $\text{TiO}_2$ ) and the  $\text{Au}_{50}\text{Pd}_{50}/\text{TiO}_2$  catalyst.

Catalyst	Surface area ( $\text{m}^2 \text{ g}^{-1}$ )	Pore volume ( $\text{cm}^3 \text{ g}^{-1}$ )
$\text{TiO}_2$	56	0.35
$\text{Au}_{50}\text{Pd}_{50}/\text{TiO}_2$	54	0.32

**Figure S3.** Au (4f) XPS spectra of  $\text{Au}_x\text{Pd}_y/\text{TiO}_2$  catalysts. From the top  $\text{Pd}/\text{TiO}_2$ ,  $\text{Au}_{35}\text{Pd}_{65}/\text{TiO}_2$ ,  $\text{Au}_{50}\text{Pd}_{50}/\text{TiO}_2$ ,  $\text{Au}_{65}\text{Pd}_{35}/\text{TiO}_2$ ,  $\text{Au}_{95}\text{Pd}_5/\text{TiO}_2$  and  $\text{Au}/\text{TiO}_2$ . Au binding energy shifts due to the addition of Pd.

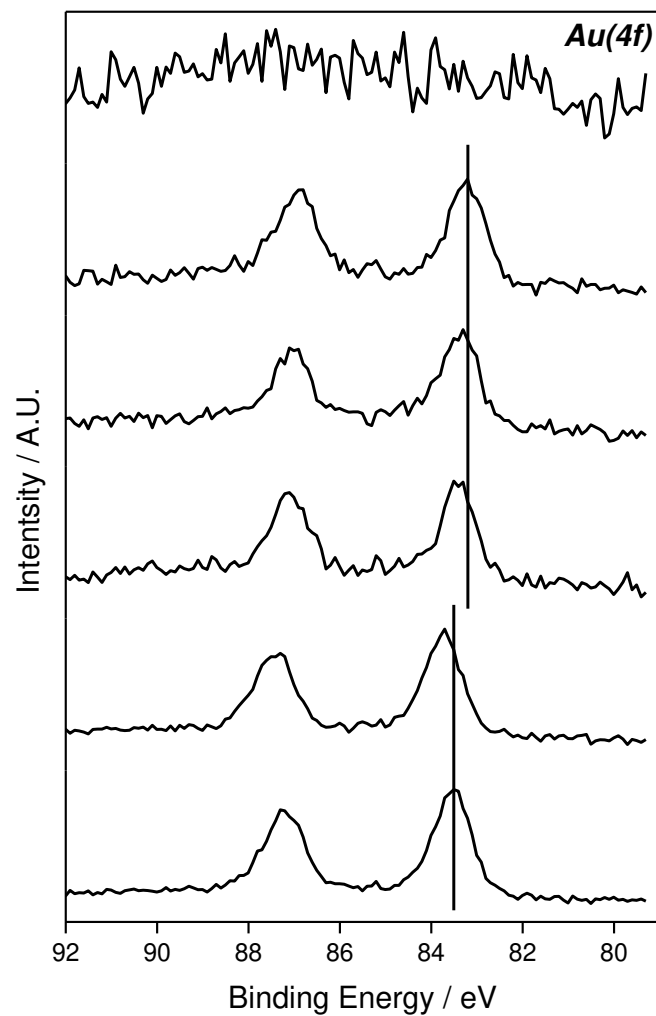


**Figure S4.** DRIFTS spectra of 1 wt% Au/TiO<sub>2</sub> after an exposure time of 1 and 10 minutes in CO/N<sub>2</sub>.

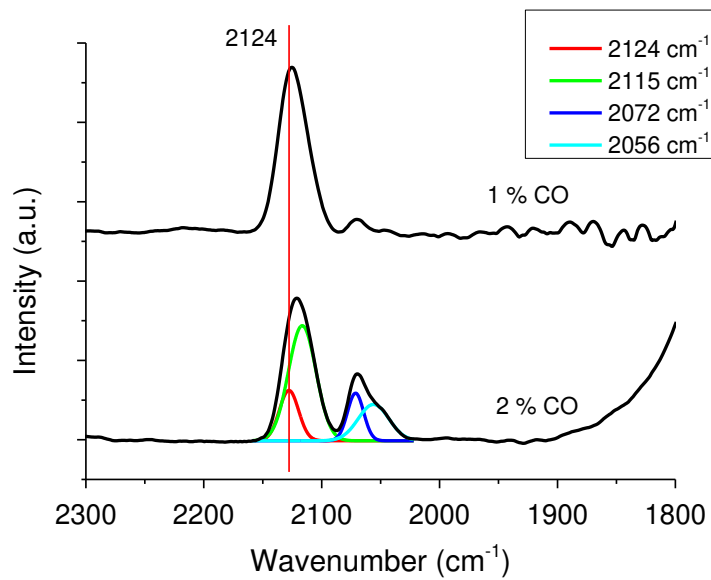


**Figure S5.** DRIFTS spectra of 1 wt% Pd/TiO<sub>2</sub> after reaching equilibrium (10 minutes) in CO/N<sub>2</sub>.

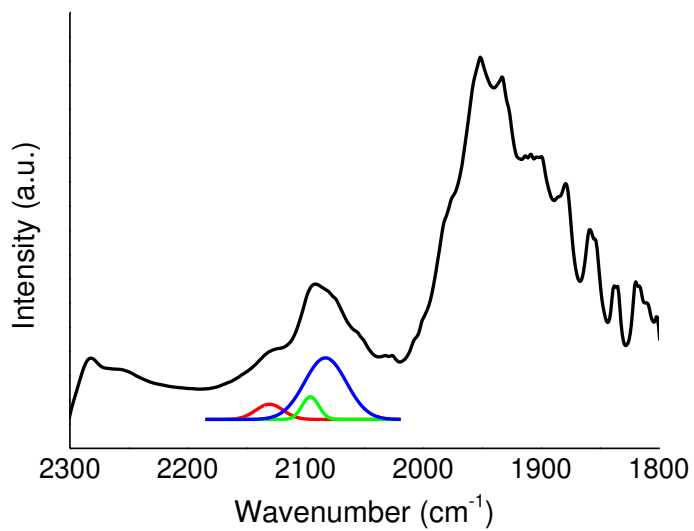


**Figure S6.** DRIFTS spectra of  $\text{Au}_{35}\text{Pd}_{65}/\text{TiO}_2$ ,  $\text{Au}_{50}\text{Pd}_{50}/\text{TiO}_2$  and  $\text{Au}_{65}\text{Pd}_{35}/\text{TiO}_2$  after reaching equilibrium (10 minutes) in  $\text{CO}/\text{N}_2$ .

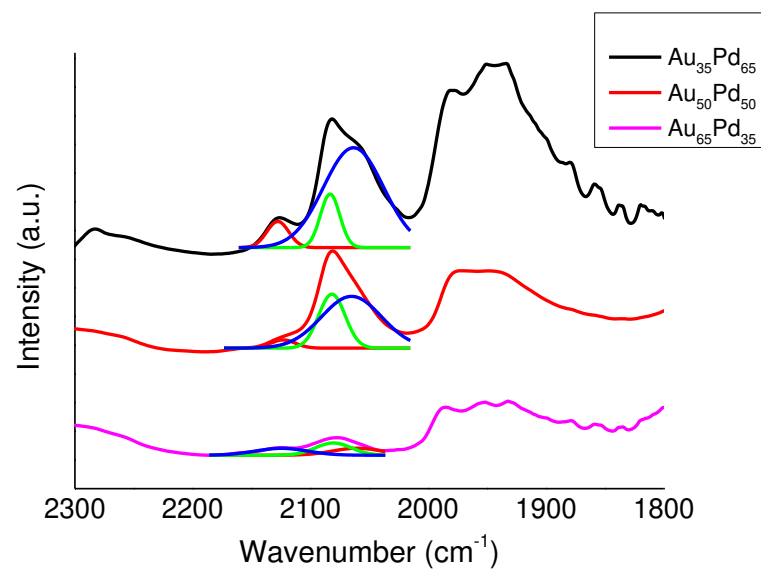


**Figure S7.** DRIFTS spectra of  $\text{Au}_{95}\text{Pd}_5/\text{TiO}_2$  after reaching equilibrium (10 minutes) in  $\text{CO}/\text{N}_2$ .

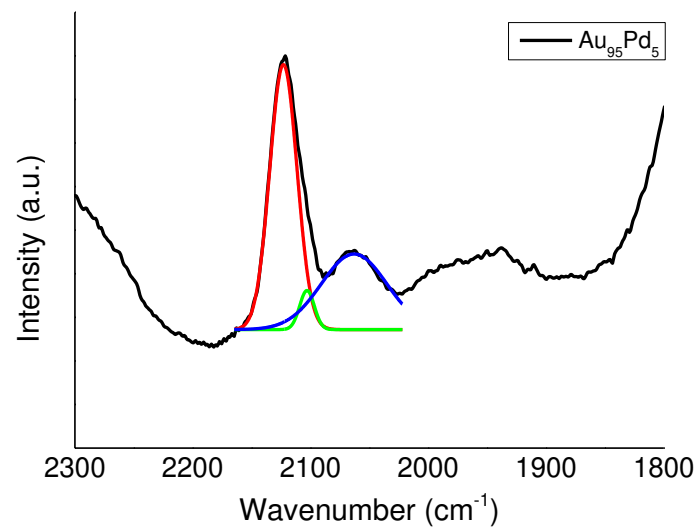


**Figure S8.** Effect of (a) stirring speed and (b) catalyst amount on the TOF of the reaction.

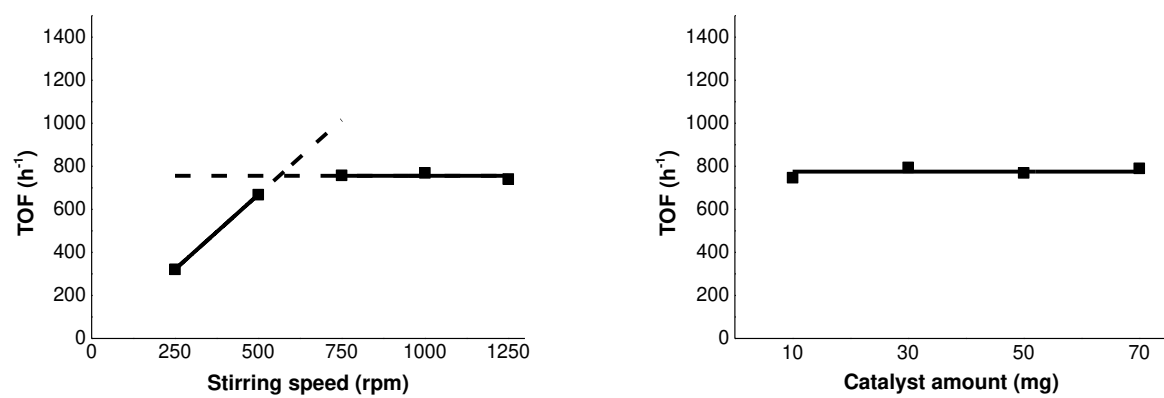


**Figure S9.** (a) Stirring effect (b) catalyst amount effect (c) temperature effect and (d) H<sub>2</sub> pressure effect on the selectivity at iso-conversion (30 % conversion).

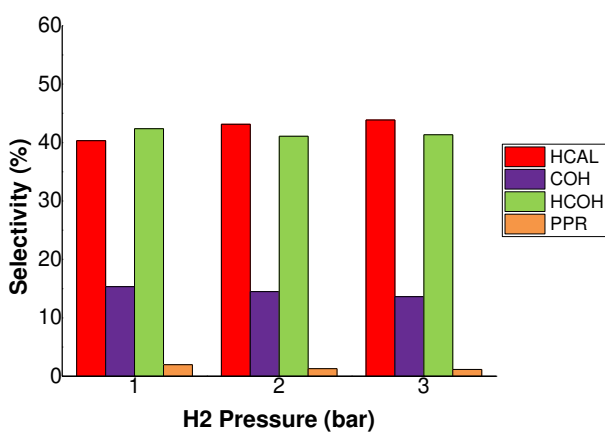
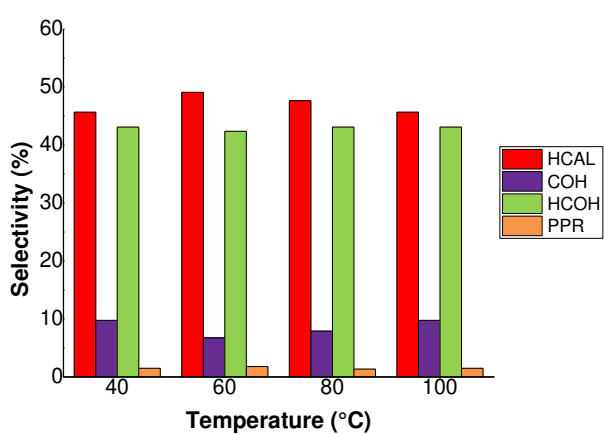
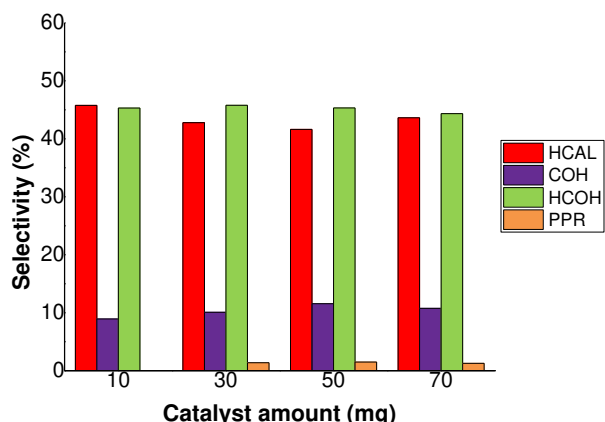
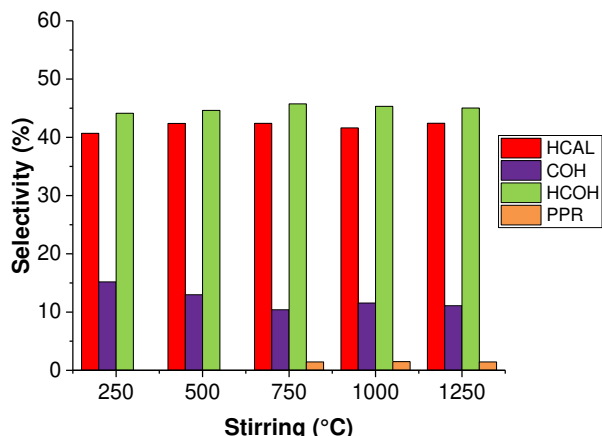


**Figure S10.** Arrhenius plot for the  $\text{Au}_{50}\text{Pd}_{50}/\text{TiO}_2$  catalyst.

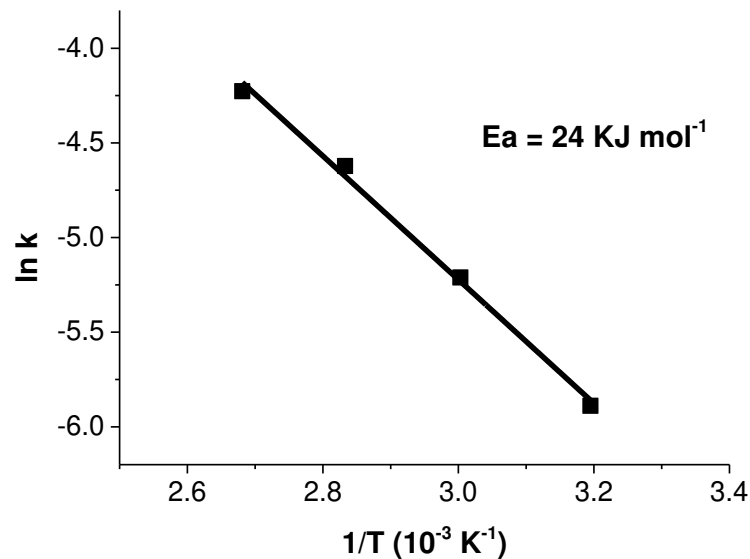


**Table S4.** Cinnamaldehyde hydrogenation activation energy for different catalysts.

Catalyst	Activation Energy (kJ mol <sup>-1</sup> )	Ref.
5 % Pd/SiO <sub>2</sub>	30.1	<sup>1</sup>
Co-B	18	<sup>2</sup>
Raney Co	35	
CoPt	17.3	<sup>3</sup>
5 % Ir/C	37	<sup>4</sup>
2 % Pt/SBA-15	21	<sup>5</sup>

**Figure S11.** FTIR analysis of the fresh and used catalyst.

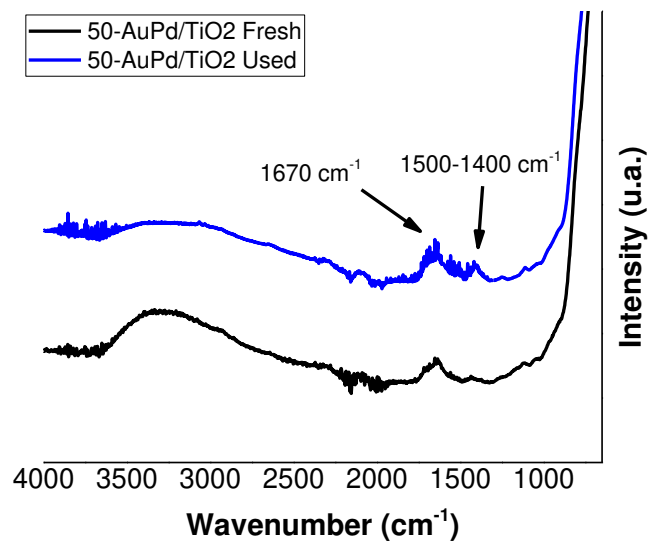


**Figure S12.** FTIR spectra of pure PVA.

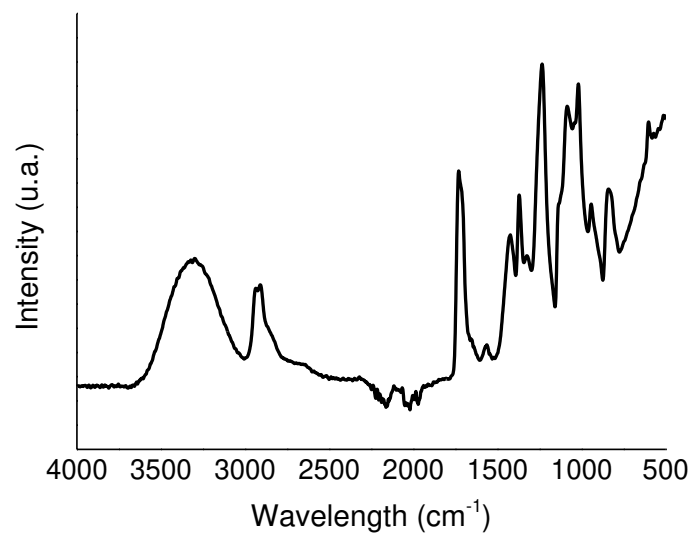


**Figure S13.** FTIR spectra of pure (a) CAL, (b) HCAL, (c) COH and (d) HCOH.

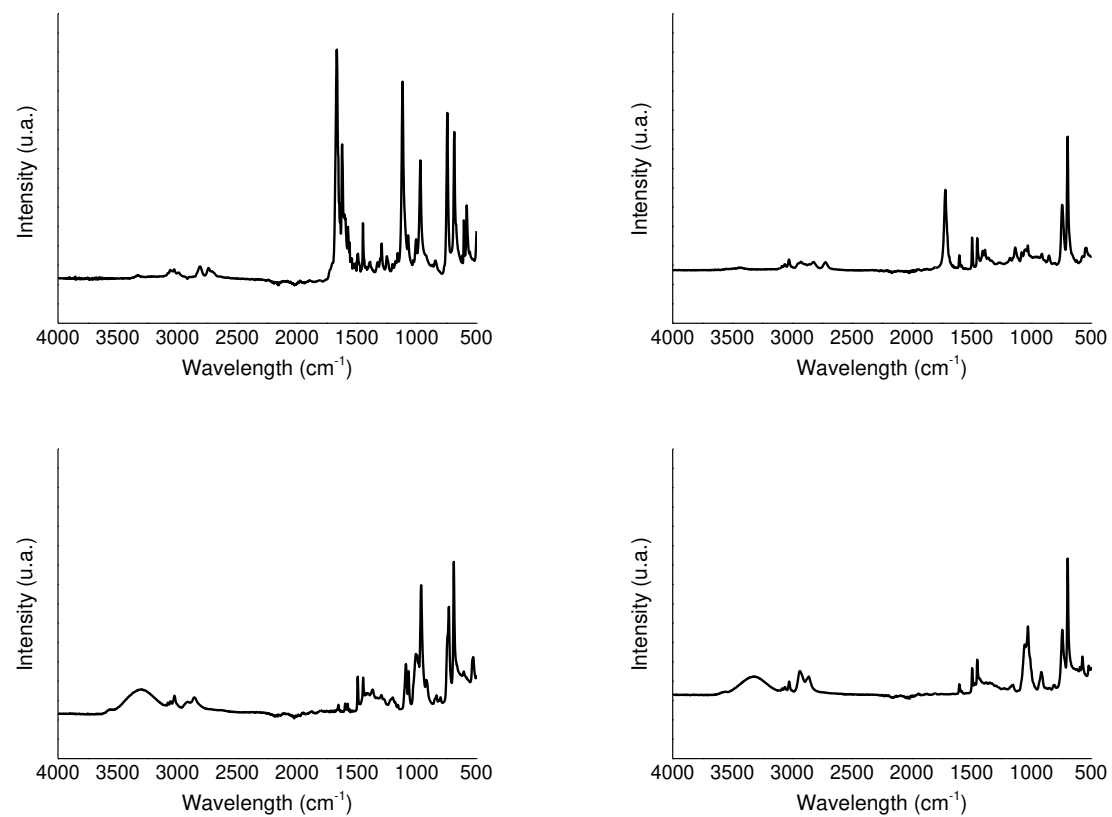


**Figure S14.** Particle size distribution of fresh and used catalysts (a) Au<sub>50</sub>Pd<sub>50</sub>/TiO<sub>2</sub> calcined at 200 °C fresh (b) Au<sub>50</sub>Pd<sub>50</sub>/TiO<sub>2</sub> calcined at 200 °C used (c) Au<sub>50</sub>Pd<sub>50</sub>/TiO<sub>2</sub> calcined at 300 °C fresh (d) Au<sub>50</sub>Pd<sub>50</sub>/TiO<sub>2</sub> calcined at 300 °C used (e) Au<sub>50</sub>Pd<sub>50</sub>/TiO<sub>2</sub> calcined at 400 °C fresh (f) Au<sub>50</sub>Pd<sub>50</sub>/TiO<sub>2</sub> calcined at 400 °C used.

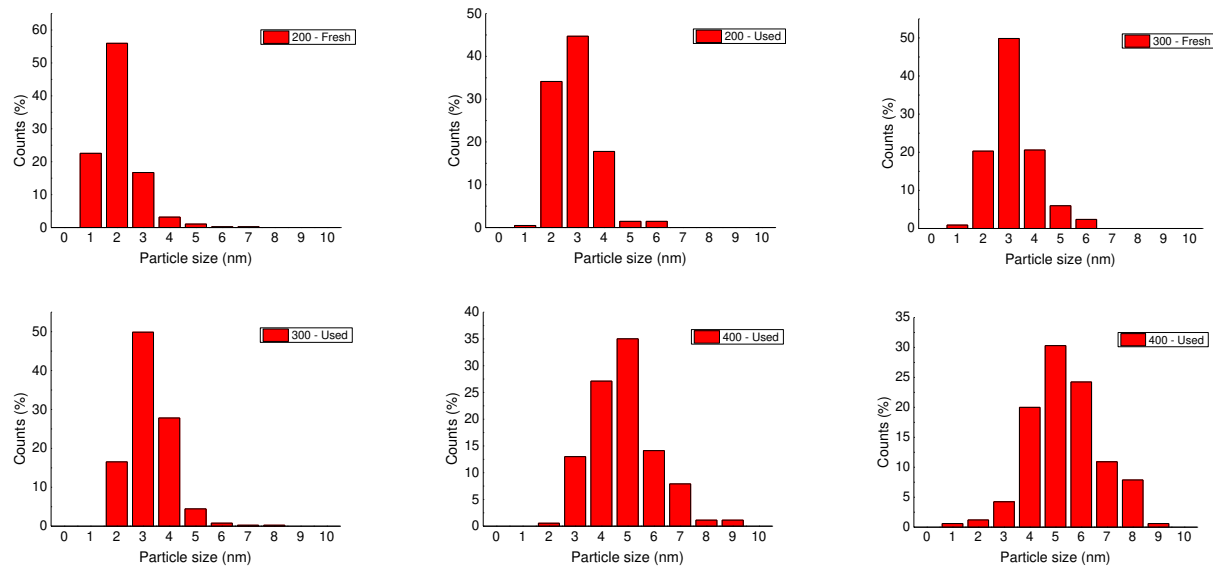


**Table S5.** XPS quantification analysis on heat treated Au<sub>50</sub>Pd<sub>50</sub>/TiO<sub>2</sub> after reaction.

Catalyst	Au/Pd ratio (mol/mol)
Au <sub>50</sub> Pd <sub>50</sub> /TiO <sub>2</sub>	47 : 53
Au <sub>50</sub> Pd <sub>50</sub> /TiO <sub>2</sub> – 200 °C Used	44 : 56
Au <sub>50</sub> Pd <sub>50</sub> /TiO <sub>2</sub> – 300 °C Used	39 : 61
Au <sub>50</sub> Pd <sub>50</sub> /TiO <sub>2</sub> – 400 °C Used	42 : 58

**Table S6.** Mean and median values obtained by TEM of Au<sub>50</sub>Pd<sub>50</sub>/TiO<sub>2</sub> catalysts in nm heat treated at different temperature.

Au <sub>50</sub> Pd <sub>50</sub> /TiO <sub>2</sub> – 200°C fresh	Au <sub>50</sub> Pd <sub>50</sub> /TiO <sub>2</sub> – 200 °C used	Au <sub>50</sub> Pd <sub>50</sub> /TiO <sub>2</sub> – 300°C fresh	Au <sub>50</sub> Pd <sub>50</sub> /TiO <sub>2</sub> – 300 °C used	Au <sub>50</sub> Pd <sub>50</sub> /TiO <sub>2</sub> – 400 °C fresh	Au <sub>50</sub> Pd <sub>50</sub> /TiO <sub>2</sub> – 400 °C used
Mean 2.5	Mean 3.2	Mean 3.7	Mean 3.8	Mean 5.3	Mean 5.9
Std-dev 0.8	Std-dev 0.8	Std-dev 1.0	Std-dev 0.8	Std-dev 1.2	Std-dev 1.3
Median 2.4	Median 3.2	Median 3.5	Median 3.7	Median 5.2	Median 5.9

**Table S7.** Activity comparison with other AuPd based catalysts reported in literature.

Catalyst	Solvent	P <sub>H2</sub> (bar)	T (° C)	TOF (h <sup>-1</sup> )	Sel <sub>H<sub>2</sub>Cal</sub> (%)	Ref.
Au <sub>50</sub> Pd <sub>50</sub>	BMIM	1	40	150	38	<sup>6</sup>
5 wt% Au <sub>56</sub> Pd <sub>44</sub> /AC	Toluene	1	22	22	38	<sup>7</sup>
1 wt% Au <sub>50</sub> Pd <sub>50</sub> /SiO <sub>2</sub>	i-Propanol	20	80	6600 <sup>a</sup>	55	<sup>8</sup>
3.5 wt% Au <sub>30</sub> Pd <sub>70</sub> /SiO <sub>2</sub>	Hexane	5	50	1200	84	<sup>9</sup>
1 wt% Au <sub>50</sub> Pd <sub>50</sub> /TiO <sub>2</sub> -300	Toluene	1	100	642	81	This study

<sup>a</sup> TOF calculated using exposed metallic surface as active site.

## Reference

- 1 S. Mahmoud, A. Hammoudeh, S. Gharaibeh and J. Melsheimer, *J. Mol. Catal. A Chem.*, 2002, **178**, 161–167.
- 2 H. Li, X. Chen, M. Wang and Y. Xu, *Appl. Catal. A Gen.*, 2002, **225**, 117–130.
- 3 W. O. Oduro, N. Cailuo, K. M. K. Yu, H. Yang and S. C. Tsang, *Phys. Chem. Chem. Phys.*, 2011, **13**, 2590–602.
- 4 J. P. Breen, R. Burch, J. Gomez-Lopez, K. Griffin and M. Hayes, *Appl. Catal. A Gen.*, 2004, **268**, 267–274.
- 5 L. J. Durndell, C. M. a. Parlett, N. S. Hondow, M. a. Isaacs, K. Wilson and A. F. Lee, *Sci. Rep.*, 2015, **5**, 9425.
- 6 P. Dash, N. A. Dehm and R. W. J. Scott, *J. Mol. Catal. A Chem.*, 2008, **286**, 114–119.
- 7 T. Szumel̄da, A. Drelinkiewicz, R. Kosydar and J. Gurgul, *Appl. Catal. A Gen.*, 2014, **487**, 1–15.
- 8 V. I. Pârvulescu, V. Pârvulescu, U. Endruschat, G. Filoti, F. E. Wagner, C. Kübel and R. Richards, *Chem. - A Eur. J.*, 2006, **12**, 2343–2357.
- 9 X. Yang, D. Chen, S. Liao, H. Song, Y. Li, Z. Fu and Y. Su, *J. Catal.*, 2012, **291**, 36–43.